Scientific Research Publishing

Journal of Computer and Communications, 2019, 7, 127-135
https://www.scirp.org/journal/jcc
ISSN Online: 2327-5227
ISSN Print: 2327-5219

Link Resource Allocation in Counter-Rotating Seam of Low-Orbit Satellite Network

Ning Li, Jiangwang Liu, Zhongliang Deng

School of Electronic Engineering, Beijing University of Posts and Telecommunications, Beijing, China
Email: lnmmdsy@bupt.edu.cn, wang6291123han@163.com, dengzhl@bupt.edu.cn

How to cite this paper: Li, N., Liu, J.W. and Deng, Z.L. (2019) Link Resource Allocation in Counter-Rotating Seam of Low-Orbit Satellite Network. *Journal of Computer and Communications*, **7**, 127-135.
https://doi.org/10.4236/jcc.2019.710012

Received: August 12, 2019
Accepted: October 9, 2019
Published: October 16, 2019

Abstract

This paper studies the communication problem at the counter-rotating seam of the low-orbit satellite based on the walker constellation. The counter-rotating seam has a short life cycle, low capacity, and dynamic geometric parameters. To better utilize the scarce link resources at the seam, increase network throughput, and approach the physical limits of the link throughput at the seam, an initial phase condition that maximizes the relative rotational joint link throughput is calculated. In the experimental simulation results using the Iridium system as an example, it is shown that better throughput can be obtained under the initial conditions, and the throughput is improved by about 30%.

Keywords

Satellite Network, Resource Allocation, Counter-Rotating Seam

1. Introduction

Large-span real-time communications under current global coverage of low-orbit satellite networks provide lower latency performance for communications than terrestrial networks. The commercial value of lower latency communication performance is enormous [1] [2]. The latency performance of low-orbit satellite networks is constrained by network architecture, network size, and so on. The network architecture mainly affects the on-board processing delay; compared with the propagation delay, the on-board processing delay is a few milliseconds. It is difficult to reduce the network delay by reducing the on-board processing delay, and the effect is limited. The size of the network reveals the latency performance limits of the system. Under the existing network scale, the network delay performance is far from the system's delay limit, and the network delay has a lot of room for reduction. The reason is that it is restricted by the dynamic counter-rotating seam.

The existing inter-satellite link does not consider the existence of a dynamic counter-rotation seam, so that the communication across the dynamic counter-rotation seam must go to the polar link, so the number of hops of the route may be greatly increased, and the delay performance of the system cannot be approximated limit. On the contrary, if the inter-satellite link at the counter-rotation seam is considered, the propagation delay of the communication may be greatly reduced, and the average network delay is reduced by nearly 50% [3]. The lack of inter-satellite links at the dynamic counter-rotation seam not only limits the delay in satellite network delay, but also limits the reliability of communication and the throughput of the network.

The lack of links at the reverse slot limits communication reliability and network throughput for a variety of reasons. The main reason for limiting the reliability of communication is that the earth's rotation leads to the rapid movement of the reverse gap coverage area (the equatorial attachment is 1677 km/h). Under such rapid movement, the switching of the satellite link near the reverse gap may lead to the delay of real-time communication service. The jitter is too large. The delay jitter in the communication process causes the receiver to compensate for the delay jitter compensation, which increases the packet loss rate and affects the reliability of the communication, and is more likely to bring a bad user experience. The main reason for the reverse gap to limit network throughput is that the bandwidth resources of the link are limited, and there is a throughput limit for a single link. Since the communication across the reverse slot must go to the polar link, and the number of polar links is much smaller than the number of links of non-reverse slot communication, the cross-slot communication is busy, which may cause the polar link load to be too large, which limits the communication throughput.

The establishment of a link at the counter-rotating seam can effectively alleviate the throughput problem of cross-slot communication. However, after the link is established, due to Doppler frequency shift, high dynamic geometry parameters, etc., the link resources are extremely limited, and the resources are the key resources to prioritize the real-time service requirements for cross-slot communication. Therefore, how to efficiently utilize the link resources in the counter-rotation seam to improve the link throughput, so that it no longer becomes a limitation of the network service capability.

2. Related Work

At present, the research on low-orbit satellite networks is becoming a hot topic in global research. How to guarantee the service capability of the network is one of the important research topics. Low-orbit satellite network routing represented by the walker constellation type is one of the research directions. This type of satellite network has a unique counter-rotation seam that constrains the improvement of network service capabilities [4].

Unbalanced flow at the reverse seam results in limited throughput, making it difficult to fully utilize link resources. The existing research on traffic imbalance is mainly focused on redistributing traffic at the network layer. The existing balancing strategy mainly adopts two methods. The first is passive processing, adaptive congestion handling. This method can alleviate the local congestion problem, but there is a cascade congestion problem, which cannot fundamentally solve the traffic imbalance problem. The second is the active processing method, load balancing. The existing load balancing routing strategy is mainly considered from the perspectives of global and local network. The strategies considered from the perspective of the network include utility maximization routing [5], time center balanced routing [6], etc.; the strategy includes agent-based load balancing routing [7], etc.; further, there are hybrid global-local load balancing routing [8] [9] considering the combination of global and local network. The above load balancing routing strategy considers load balancing for measurable node throughput, node processing capability, delay, route hop count, network utilization, and link bandwidth capacity. However, the above routing strategies are difficult to adapt to the unique link characteristics at the reverse slot, so they are not suitable for dealing with the traffic imbalance problem at the reverse slot.

The characteristics of short link generation time, extremely limited resources, and high dynamics at the counter-rotating seam directly affect the quality of service of real-time services across the gap communication. The link resources should give priority to real-time services. One of the reasons for the imbalance of traffic distribution is that due to the unbalanced distribution of access devices, we actively cater to this imbalance from the physical level and redistribute the link resources to achieve efficient use of limited link resources. Next, we describe its research ideas from three aspects. The third part describes the network model at the reverse joint. The fourth part analyzes the link resource status and initial conditions. The fifth part is completed. The fourth part is the simulation verification of theoretical analysis.

3. LEO Satellite Network Counter-Rotating Seam (CRS) Model

We use a Walker constellation composed of N orbits. Each orbital plane has M satellites evenly distributed, and the adjacent orbital planes have a phase difference of π/M. We assume that in this constellation, the dip is 90˚. The intersection angle of these planes is 185˚/N, but the angle of the plane at the counter-rotating joint (dashed line) is smaller to ensure no dead angle coverage at the seam, intersecting only near the north and south pole regions. For ease of reference, only two orbital planes at the reverse seam are shown in **Figure 1**, and the M satellites in each orbital plane are separated from each other by an angular distance of 360˚/M. The red arrow in the figure represents the direction of satellite movement in the two hemispheres bounded by the seam. This paper mainly introduces the counter-rotation seam and some related basic concepts.

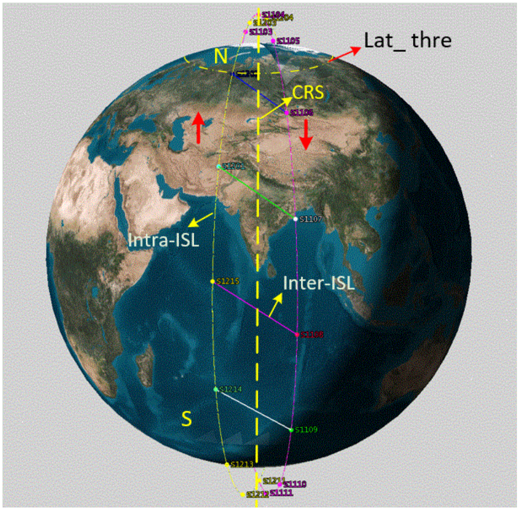

Figure 1. Topology of LEO satellite network counter-rotating seam model.

Logical location: Satellites can be identified by logical locations. The earth's surface is broken down into a regular honeycomb structure. Each unit of the unit structure has its own identifier called a logical location. The logical location does not change and is appended to its nearest satellite as its location address or identifier. A satellite serving a logical location has the same identifier as the unit it serves. The logical position of the satellite is expressed as <C, R>, where C = 0, 1, 2... N − 1 represents the plane position of the satellite, and R = 0, 1, 2... M − 1 represents the satellite mark in the orbital plane. The routing algorithm can be based on a virtual topology consisting of these logical locations. This way we don't need to pay too much attention to satellite mobility during the routing process.

Latitude threshold (Lat_thre): The yellow dotted line in the polar region of the figure represents the latitude threshold. When the satellite's sub-satellite trajectory intersects the threshold line, it represents the current satellite's Inter-ISL link failure.

Counter-Rotating Seam (CRS): There are two special longitudinal zones where the direction of rotation of the adjacent planes is reversed. The boundary of the anti-rotation plane is called the anti-rotation slot (CRS). As shown in Figure 1, due to the high-speed mobility of the satellite, the communication link between the satellites is difficult to maintain through the CRS.

Satellite Inter-satellite Link (ISL): These satellites are interconnected by ISL. The propagation delay between two neighbors depends to a large extent on the length of the ISL. Calculate the average ISL length L_v (*i.e.* Intra-ISL) in the plane:

$$L_v = \sqrt{2} * R\sqrt{1 - \cos\left(\frac{360^\circ}{M}\right)} \tag{1}$$

where R is the plane radius. The length of the link changes rapidly due to the relatively high speed movement of the satellite at the seam. Therefore, the inter-satellite link length between adjacent track planes at the seam is L_h (*i.e.* Inter-ISL):

$$L_h = \sqrt{2} * R\sqrt{1-\cos(\alpha)} * \frac{\cos(H_{lat})}{\cos(\Delta lat)} \tag{2}$$

where α is the angle of the adjacent orbital plane at the joint, H_{lat} is the latitude of the low-latitude satellite node in Inter-ISL, and Δlat is the latitude difference of the satellite nodes at the two ends of the Inter-ISL.

4. Initial Phase Conditions for Maximizing Throughput

4.1. Inter-Satellite Link Feature at the Counter-Rotating Seam

The satellite link at the counter-rotating seam has a short life cycle and low capacity, and there is a latitude threshold between the inter-satellite links between adjacent orbital planes. The inter-satellite link at the seam considers that the Inter-ISL of the satellite node fails when the sub-satellite trajectory intersects the threshold plane and goes to the polar region. As shown in **Figure 2**, the figure is a track cutaway view of the counterclockwise movement at the seam, wherein the broken line represents the latitude threshold Φ (0 < Φ < π/2) or the equatorial plane; The solid line from the center of the circle to the circle represents the satellite node and its inter-satellite link within the latitude threshold; α, β, θ, γ are the closest to the latitude threshold and the angle between the satellite node with the link and the threshold surface; 1 and 2 represent the case where M is even, 3 and 4 represent the case where M is an odd number (the calculation process can be referred to [10] [11]).

When the number of satellite orbital planes is N, the number of satellites in the orbital plane is M, and the latitude threshold Φ is a fixed value, since the spatial distance between two adjacent Inter-ISL links at the counter-rotating seam is a fixed value L_v, it can be proved The number of links at the seam is N_{C_ISL}:

$$N_{C\_ISL} = \begin{cases} 2*\left\lceil \frac{\Phi * M}{\pi} \right\rceil, & \alpha+\beta \le \frac{2\pi}{M}, \theta+\gamma \le \frac{2\pi}{M} \\ 2*\left\lfloor \frac{\Phi * M}{\pi} \right\rfloor, & \alpha+\beta > \frac{2\pi}{M}, \theta+\gamma > \frac{2\pi}{M} \\ 2*\left\lceil \frac{\Phi * M}{\pi} \right\rceil - 1, & \left(\alpha+\beta \le \frac{2\pi}{M}, \theta+\gamma > \frac{2\pi}{M}\right) \cup \left(\alpha+\beta > \frac{2\pi}{M}, \theta+\gamma \le \frac{2\pi}{M}\right) \end{cases} \tag{3}$$

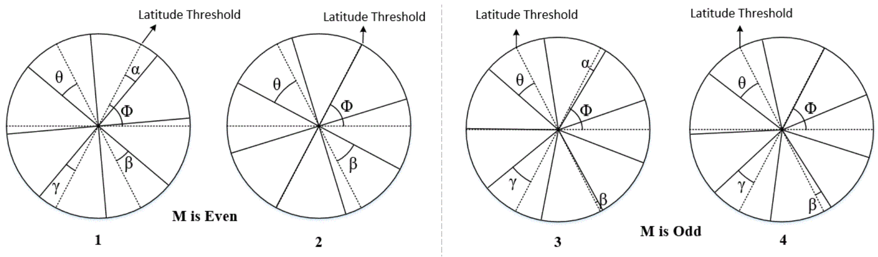

Figure 2. Track section diagram.

It can be seen from N_{C_ISL} that when N, M, and Φ are constant values, the periodic motion of the satellite nodes causes the number of links to also exhibit discrete periodic fluctuations, and the duration of a single link also exhibits periodicity feature. Therefore, the total link duration at the seam at each cycle is a constant value T.

4.2. Initial Phase Conditions That Maximize Throughput at the Counter-Rotating Seam

When the conditions such as the number of satellites, bandwidth, and latitude threshold are fixed, the network throughput capability is positively correlated with the link resources, and the link resources are positively correlated with the number of links and link duration. It can be known from A that the number of links and the total link duration are constant values, that is, the link resources are fixed values. On this basis, the distribution of resources directly affects network throughput. Due to factors such as the population, the density of access equipment, and the diversity of service traffic requirements, the distribution of traffic in the satellite network access network is uneven. Obviously, the population and access equipment in the northern hemisphere are more dense, so the long duration of the northern hemisphere link helps to increase network throughput.

As shown in **Figure 3**, the circular area represents the coverage area of the satellite node, the thick line arrow represents the orbit of the joint movement at the seam, the solid line between the tracks represents the real link, and the dotted line represents the virtual link that will become the actual link. **Figure 3** shows the special link state at the seam, assuming it is the initial state, making it easy to calculate the initial phase corresponding to maximizing the duration of the Northern Hemisphere link. Analysis of **Figure 2** and **Figure 3** can be proved that the remaining phase is ρ and the optimal initial phase is φ $(0 < \varphi < \pi/M)$:

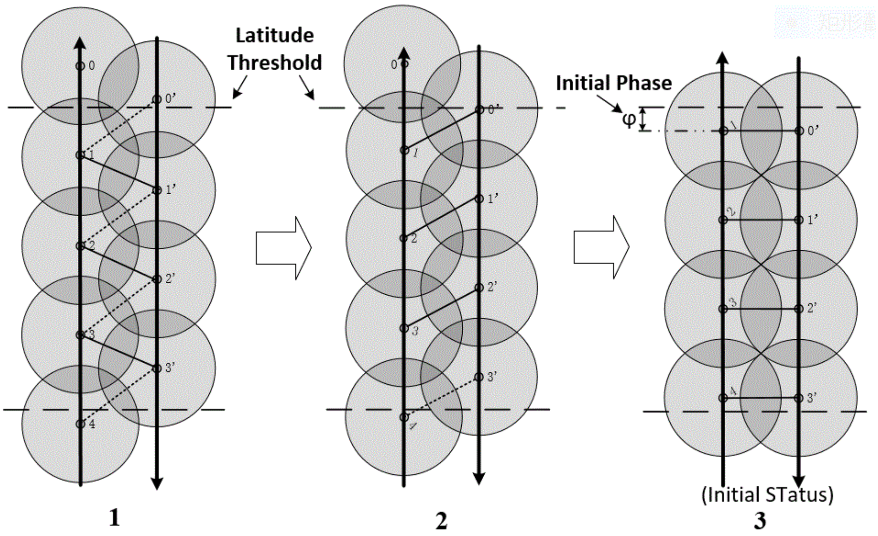

Figure 3. Counter-rotating Seam link initial phase condition.

$$\rho = 2*\Phi - \left\lfloor \frac{\Phi*M}{\pi} \right\rfloor * \frac{2*\pi}{M} \tag{4}$$

$$\varphi = \begin{cases} \dfrac{\rho}{2}, & M = 2n \cup \dfrac{\pi}{M} \le \rho < \dfrac{\pi}{2*M} \\ \dfrac{\pi}{2*M}, & \dfrac{\pi}{M} \le \rho < \dfrac{\pi}{2*M} \\ \rho, & 0 \le \rho < \dfrac{\pi}{2*M} \end{cases} \tag{5}$$

Proof:

1) When M is even, the initial phase of the optimal link assignment is $\varphi = \rho/2$ due to symmetry. The value is the mean value, that is, the link duration of the north and south hemispheres is the same.

2) When M is an odd number, the initial phase has a value range of $0 \le \varphi < 2\pi/M$. And $\theta + \alpha = \gamma + \beta$ is always true, $\alpha + \beta = \rho$ or $\alpha + \beta = \rho + 2\pi/M$ is always true, $0 \le \rho < 2\pi/M$, which can be proved by the above conditions combined with **Figure 3**.

Changes in the initial phase conditions will inevitably lead to phase changes in other orbits, but have no effect on the number and duration of inter-satellite links.

5. Simulation and Performance Evaluation

We use STK and Opnet software for joint simulation. Under the simulated Iridium system model (M = 11), we evaluate the optimal phase condition φ and $\varphi = \rho/2$ throughput comparison under phase conditions ($\Phi = 70^\circ$). The satellite node traffic rate is satisfied as shown in **Figure 4**. This figure shows the distribution density of global IoT devices. We assume that the node traffic demand is proportional to the device density:

Simulation condition and results: The simulation conditions and their results are shown in **Figures 5**, the length of the data packet crs_packet is fixed to 1024 bits, and the simulation time is 20 minutes.

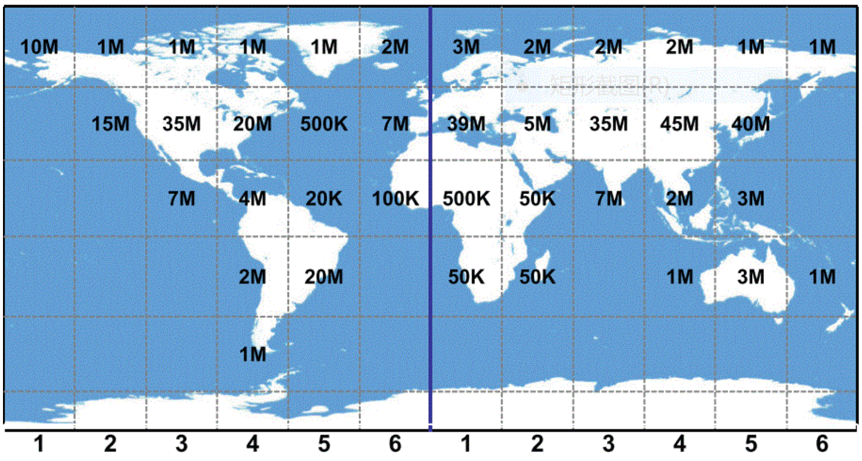

Figure 4. Earth zone division and IoT device density.

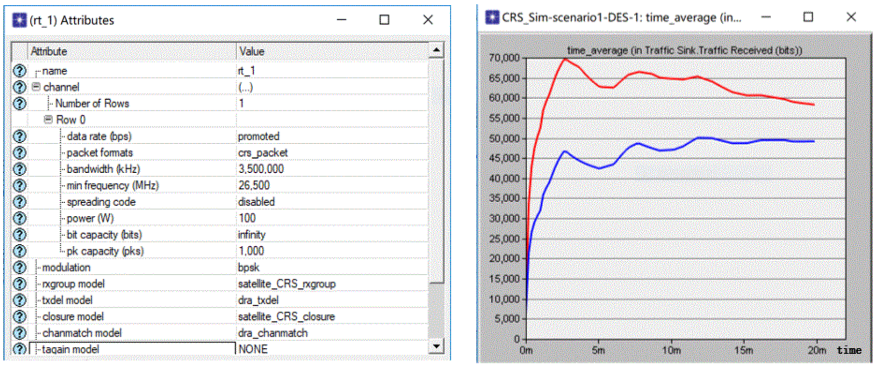

Attribute	Value
name	rt_1
channel	(...)
Number of Rows	1
Row 0	
data rate (bps)	promoted
packet formats	crs_packet
bandwidth (kHz)	3,500,000
min frequency (MHz)	26,500
spreading code	disabled
power (W)	100
bit capacity (bits)	infinity
pk capacity (pks)	1,000
modulation	bpsk
rxgroup model	satellite_CRS_rxgroup
txdel model	dra_txdel
closure model	satellite_CRS_closure
chanmatch model	dra_chanmatch
tagain model	NONE

Figure 5. Simulation condition and throughput simulation results.

As shown in **Figure 5**, there is a throughput comparison graph for two phase conditions, where red represents the throughput under optimal phase conditions. Compared to the average condition ($\varphi = \rho / 2$) it throughput increased by nearly 30%.

6. Conclusions and Future Work

Aiming at the link resource allocation problem at the counter-rotating seam of the low-orbit satellite network, we carefully analyzed the distribution characteristics of the link resources and calculated the optimal initial phase condition φ. Based on the Iridium system model, the simulation verified that the link throughput at the joint is improved by about 30% under the optimal phase condition, which is in line with the theoretical analysis results in Section IV. Next, In order to solve the impact of the reverse rotation gap on the service quality of the communication service, such as delay, jitter and reliability, it is necessary to pay attention to the network topology and routing related issues as a further research direction future.

Conflicts of Interest

The authors declare no conflicts of interest regarding the publication of this paper.

References

[1] Cisco (2019) White Paper: Cisco Visual Networking Index: Global Mobile Data Traffic Forecast Update, 2017-2022.

[2] Cisco (2018) White Paper: Cisco Global Cloud Index: Forecast and Methodology, 2016-2021.

[3] Guo, Z. and Yan, Z. (2015) A Weighted Semi-Distributed Routing Algorithm for LEO Satellite Networks. *Journal of Network and Computer Applications*, 1-11. https://doi.org/10.1016/j.jnca.2015.08.015

[4] Yeo, B.S. (2004) An Approach to the Modeling of Counter-Rotating Seam Communication Links for LEO Satellite Systems. *IEEE Wireless Communications and Networking Conference*, 1-4. https://doi.org/10.1109/wcnc.2004.1311395

[5] Yong, L., Jun, Z. and Tao, Z. (2015) UMR: A Utility-Maximizing Routing Algo-

rithm for Delay-Sensitive Service in LEO Satellite Networks. *Chinese Journal of Aeronautics*, 499-507. https://doi.org/10.1016/j.cja.2015.01.001

[6] Zhang, Z. (2018) Temporal Centrality-Balanced Traffic Management for Space Satellite Networks. *IEEE Transactions on Vehicular Technology*, **67**, 4427-4439. https://doi.org/10.1109/tvt.2017.2787761

[7] Rao, Y. and Wang, R.-C. (2010) Agent-Based Load Balancing Routing for LEO Satellite Networks. *Computer Networks*, 3187-3195. https://doi.org/10.1016/j.comnet.2010.06.019

[8] Liu, Z.L., Li, J.S. and Wang, Y.R. (2017) HGL: A Hybrid Global-Local Load Balancing Routing Scheme for the Internet of Things through Satellite Networks. *International Journal of Distributed Sensor Networks*, **13**. https://doi.org/10.1177/1550147717692586

[9] Liu, P., Chen, H.Y. and Wei, S.J. (2018) Hybrid-Traffic-Detour Based Load Balancing for Onboard Routing in LEO Satellite Networks. *China Communications*, 28-41. https://doi.org/10.1109/cc.2018.8398222

[10] Lu, Y. (2013) Virtual Topology for LEO Satellite Networks Based on Earth-Fixed Footprint Mode. *IEEE Communications Letters*, 357-360. https://doi.org/10.1109/lcomm.2013.011113.122635

[11] Wang, J.F. (2007) Topological Dynamics Characterization for LEO Satellite Networks. *Computer Networks*, 43-53.